*J. Fluid Mech.* (1981), *vol.* 113, *pp.* 513–529
*Printed in Great Britain*



# Radial fingering in a Hele Shaw cell

By LINCOLN PATERSON

Department of Engineering Physics, Research School of Physical Sciences,
The Australian National University, Canberra, 2600, Australia

(Received 29 April 1981)

The results of experiments involving instability, known as fingering, in a circular Hele Shaw cell with inward and outward flow are presented. The width of fingers in this situation is examined, and an approximate equation for the growth of fingers is proposed. The equation $r^{\alpha} = \cos(n\theta)$ is shown to fit the shape of long fingers.

## 1. Introduction

When one fluid displaces another in a porous medium, the displacement can be either stable or unstable. If the displacement is unstable, long 'fingers' of the displacing fluid can penetrate into the displaced fluid. This phenomenon is known as fingering. (See, for example, Richardson 1961.) In horizontal flow, fingering occurs when a less viscous fluid displaces a more viscous fluid. Viscous fingering is not established as a real phenomenon at reservoir conditions (Settari, Price & Dupont 1977). However, there have been a number of experiments with models that have established it as a phenomenon in the laboratory (for example, van Meurs 1957; Habermann 1960).

The Hele Shaw cell is a device for investigating two-dimensional flow in porous media. It is based on the similarity between the differential equations governing saturated flow in a porous medium and those describing the flow of a viscous fluid in the narrow space between two parallel planes. Linear fingering in a Hele Shaw cell is a subject that has been studied by many authors (for example, Saffman & Taylor 1958; Chuoke, van Meurs & van der Poel 1959; Wooding 1969; Gupta, Varnon & Greenkorn 1973; White, Colombera & Philip 1976; Pitts 1980).

Linear fingering refers to fingering that occurs with a linear displacement and an initially planar interface. One of its main sources of interest is the oil industry, where it reduces the amount of oil which is economically recoverable. In practice, when fluids are injected into the ground, they are injected through a well which, in effect, is a point source. Displacement (initially at least) is in the radial direction. One would therefore consider the radial model to be more appropriate to practical situations than the linear displacement model. Bataille (1968) and Wilson (1975) have both considered the linear perturbation analysis for a circular interface in a Hele Shaw cell, but neither author has gone far beyond this.

The dual motivation behind this study is its relevance to the underground storage of gas (Carden & Paterson 1979; Paterson 1980) and to the recovery of oil. Hence, both outward fingering (gas injection) and inward fingering (oil recovery) are examined. The growth of fingers is examined in four stages: the initial growth, intermediate growth, quasi-infinite fingers and extended growth and splitting. The significant

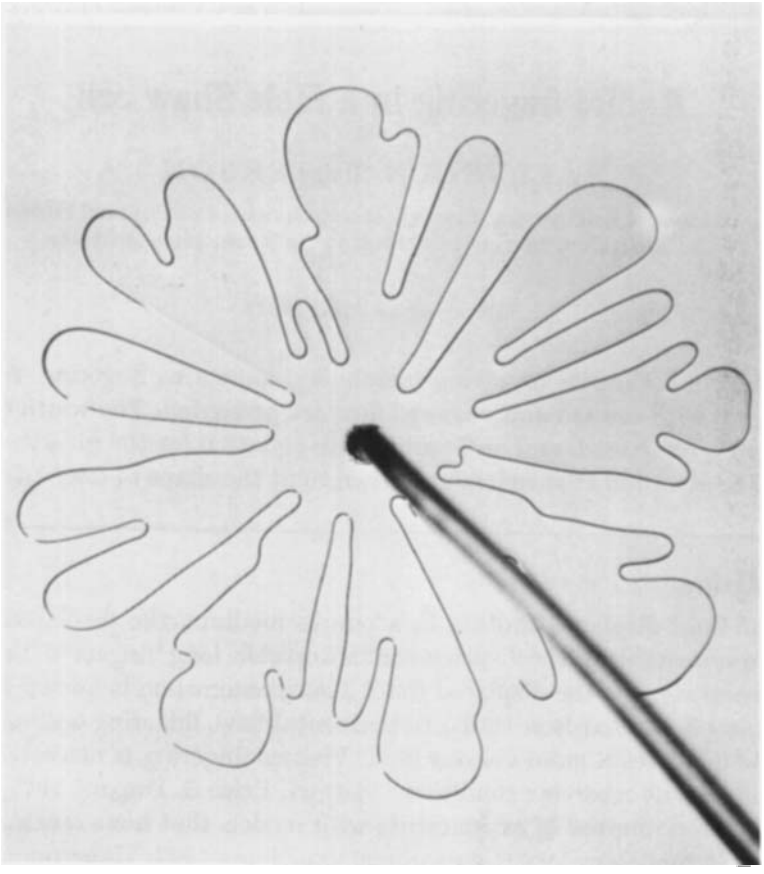

FIGURE 1. The pattern which occurs after the injection of air into a Hele Shaw cell filled with glycerine.

results of this paper are the examination of the minimum wavelength of a finger in the radial situation, the derivation of an approximate form of the growth rate of the fingers and the derivation of the equation describing the shape of a long finger. These results are compared with Hele Shaw cell experiments which are typified in figure 1 by a pattern which resulted from the injection of air into a Hele Shaw cell filled with glycerine.

## 2. Apparatus

For a discussion on the relevance of Hele Shaw cells to flow in porous media, the reader is referred to the papers on linear fingering cited above and to Bear (1973). It must be acknowledged that their relevance is not completely certain, as pointed out by Wooding & Morel-Seytoux (1976) in an article which contains a review of linear fingering.

The essential parts of the circular Hele Shaw cell used in the experiments consisted of two 13 mm thick glass disks, 600 mm in diameter, spaced a few millimetres apart. A system of screws, sprockets and a chain was used to change the spacing between the disks while keeping them parallel. A hole was drilled in the centre of one of the disks so

that fluids could be injected and withdrawn. With the disks very close together, a sodium lamp was used to determine the deviations in spacing by creating interference fringes which were then counted. The disks had a variation in spacing of about 0·05 mm. Most experiments were conducted with a plate spacing of 1·50 mm. During an experiment, pressure changes caused the disks to flex slightly, introducing some additional variation in spacing. Strain calculations (from Roark 1965) indicated that the additional variations in spacing should be less than 0·1 mm for the regions of interest in the experiments.† At the outer perimeter of the disks a retainer maintained a uniform head of liquid.

## 3. Outward fingering

### 3.1. *Initial growth*

The outward flow experiments commenced with the Hele Shaw cell filled with the more viscous fluid. The less viscous fluid was then injected at the centre at a constant rate, forming an initially circular interface when viewed from above. As the bubble developed, the interface began to finger. The criteria for this will now be discussed.

Chuoke *et al.* (1959), Scheideggar (1960*a*, *b*) have made studies of the initial growth of fingers from a linear interface. In particular, Chuoke *et al.* have shown that surface tension prevents fingers from occurring below a certain wavelength, where wavelength is defined as peak-to-peak separation.

The problem of the instability of an initially circular interface has been examined elsewhere (Bataille 1968; Wilson 1975). Since the analysis is illustrative and beneficial to the subsequent analysis, a version of the derivation will be included here.

Darcy's law is the equation governing the velocity of flow $\mathbf{v}$ in a porous medium or a Hele Shaw cell as a function of pressure $p$,

$$\mathbf{v} = -M\nabla p, \tag{1}$$

where $M$ is the fluid mobility. Mobility in a Hele Shaw cell is a function of the plate spacing $b$ and the fluid viscosity $\mu$:

$$M = b^2/12\mu. \tag{2}$$

In the problem under consideration, the subscripts 1 and 2 will be used to refer to the inner and outer fluids respectively. For incompressible flow, Darcy's law in polar co-ordinates leads to

$$\frac{\partial^2\phi_j}{\partial r^2}+\frac{1}{r}\frac{\partial\phi_j}{\partial r}+\frac{1}{r^2}\frac{\partial^2\phi_j}{\partial\theta^2}=0, \tag{3}$$

where $\phi_j = M_j p_j$ is the velocity potential.

Part of a circular interface with a sinusoidal perturbation is shown in figure 2. The source has volume flow rate $Qb$ and the circle has radius $R$, so that, for unperturbed displacements,

$$R(t) = (Q(t-t_0)/\pi)^{\frac{1}{2}}, \tag{4}$$

if $R = 0$ at $t = t_0$. For both inflow and outflow, $Q(t-t_0) > 0$. The velocity potential of the steady flow can be derived from (3) as

$$\phi_j^{(0)} = -\frac{Q}{2\pi}\left[\ln\frac{r}{R}+\frac{M_j}{M_2}\right], \tag{5}$$

† Using equation (15), it is possible to show that this variation in spacing will cause less than 7 % variation in the width of fingers: certainly well within the realm of the statistical variations.

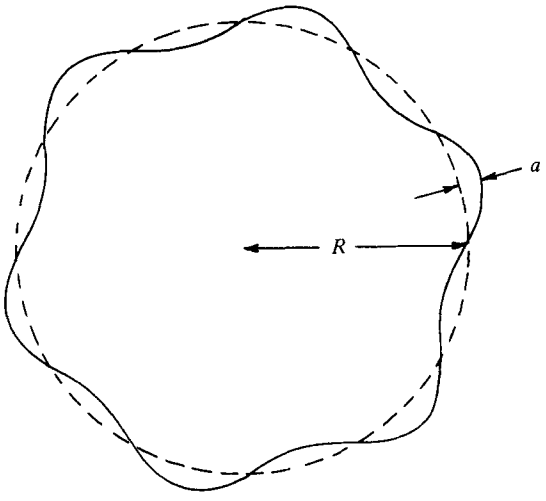


FIGURE 2. A circular interface of radius $R$ with a wavelike perturbation $a$.

which satisfies the continuity of pressure and radial velocity at the interface $r = R(t)$.

As the interface moves, it experiences perturbations due to inhomogeneities. Any perturbation can be expressed as an infinite sum of wavelike functions. For the purpose of the following linear analysis, it is sufficient to consider a single wavelike perturbation $a$ with amplitude $A$, as shown in figure 2, so that

$$a = Af(t)\exp(in\theta), \quad n = 1, 2, 3, \ldots, \tag{6}$$

where $f(t)$ represents the dependence of the amplitude on time.

The required solution of (3), with $\beta$ to be determined, is

$$\phi_j = \phi_j^{(0)} + (-1)^j \beta \left(\frac{r^n}{R^n}\right)^{(-1)^{j-1}} \exp(in\theta). \tag{7}$$

The condition of continuity at the perturbed interface (to first order at $r = R(t)$) determines $\beta$ as

$$\beta = \frac{A}{n}\left(\frac{Qf}{2\pi R} + R\frac{df}{dt}\right) \tag{8}$$

The pressure drop across the interface depends on the surface tension $\sigma$ through

$$p_1 - p_2 = \sigma\left(\frac{2}{b} + \frac{1}{R} - \frac{a + d^2a/d\theta^2}{R^2}\right) \tag{9}$$

to first order, since $r = R + a$. Using (5)–(9) gives

$$\frac{1}{f}\frac{df}{dt} = \frac{Qn}{2\pi R^2}\left[\frac{M_1 - M_2}{M_1 + M_2}\right] - \frac{Q}{2\pi R^2} - \frac{\sigma n(n^2-1)}{R^3}\left[\frac{M_1 M_2}{M_1 + M_2}\right]. \tag{10}$$

If $M_1 \gg M_2$, (10) becomes

$$\frac{df}{dt} = \frac{n-1}{R^2}\left(\frac{Q}{2\pi} - \frac{n(n+1)\sigma M_2}{R}\right) f. \tag{11}$$

The condition $df/dt = 0$ gives rise to a minimum wavelength $\lambda_c$ for a perturbation to be maintained. With this condition, (11) can be solved for $n$ to give

$$n_c = \left[\frac{QR}{2\pi M_2 \sigma} + \tfrac{1}{4}\right]^{\frac{1}{2}} - \tfrac{1}{2}. \tag{12}$$

Since $n = 2\pi R/\lambda$, this gives the critical wavelength $\lambda_c$ as

$$\lambda_c = 2\pi R \Big/ \left\{ \left( \frac{QR}{2\pi M_2 \sigma} + \tfrac{1}{4} \right)^{\frac{1}{2}} - \tfrac{1}{2} \right\}. \tag{13}$$

Maximum growth occurs when

$$\frac{\partial}{\partial n}\left(\frac{df}{dt}\right) = 0,$$

which, from (11), is

$$n_m = \left[ \frac{1}{3} \left( \frac{QR}{2\pi M_2 \sigma} + 1 \right) \right]^{\frac{1}{2}}, \tag{14}$$

or substituting $n = 2\pi R/\lambda$ leads to a wavelength of maximum growth rate, $\lambda_m$:

$$\lambda_m = 2\sqrt{3}\,\pi R \Big/ \left( \frac{QR}{2\pi M_2 \sigma} + 1 \right)^{\frac{1}{2}}. \tag{15}$$

The net result is as follows. One would expect that, when the circumference of the injected 'bubble' is less than the critical wavelength, the displacement is stable and the interface remains a circle centred on the injection point. Once the circumference is greater than this wavelength, fingers are able to grow with the fastest-growing incipient fingers having wavelength $\lambda_m$.

Figure 3 is a multiple exposure photograph of a 'bubble' growing. In this example $Q = 9{\cdot}3\ \mathrm{cm^2/s}$; $b = 0{\cdot}15$ cm and $\sigma = 63$ dyne/cm. The temperature was 28 °C at which $M_2 = 3{\cdot}6 \times 10^{-4}\ (\mathrm{cm^4/dyne})/\mathrm{s}$. Using (15), $\lambda_c$ and $\lambda_m$ have been plotted as a function of $R$ at the same scale as the photograph. The exposures occurred at 0·3 Hz. Inspection of the photograph reveals that the fingers appear to have wavelength $\lambda_m$ at their inception. During the time the fingers develop, their wavelength becomes greater than $\lambda_m$, but this is now beyond the realm of the stability theory considered above.

### 3.2. *Intermediate growth*

The subject of intermediate growth does not appear to have been tackled previously as a whole, presumably because of the difficult mathematics involved. In this paper the problem is approached by making a number of assumptions. These assumptions are shown to lead to a good empirical fit with experiment.

3.2.1. *Theory and assumptions.* Some previous work has been done on aspects of the growth rate of fingers from a planar interface. Saffman (1959) and Scheideggar (1960*a*) have both presented calculations that indicate that a finger grows exponentially at its conception. For large $t$, Saffman has also shown that it is expected that the growth velocity will become constant. Gupta *et al.* (1973) have done experiments in which the growth velocity of fingers is constant with time.

These results prompt the following conjectured solution for the length of a finger $L$ in the linear situation:

$$L = 2k' \ln (1 + k'' e^{t/k'}), \tag{16}$$

where $k'$ and $k''$ are to be determined. A next assumption could be to set the finger width equal to the finger spacing. This is reasonable in the light of the results of Saffman & Taylor (1958) and further backed up by Pollard, Muller & Dockstad (1975). The latter work refers to fingers of igneous rock intruding into a sandstone–shale host. Let the extreme point of an advancing finger be referred to as the 'tip' and the

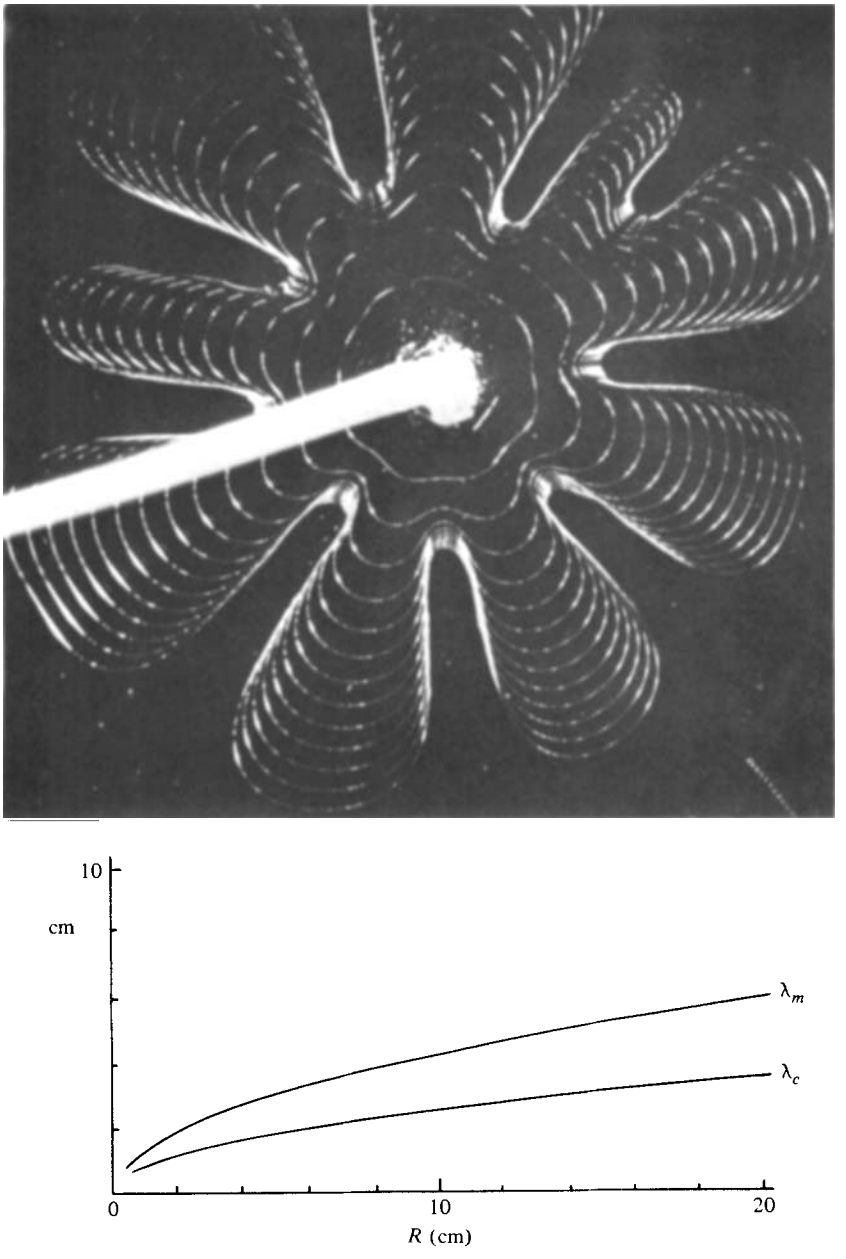


FIGURE 3. A multiple exposure photograph taken during the injection of air into a Hele Shaw cell filled with glycerine.

extreme point of the withdrawing fluid be referred to as the 'base' of the finger. The finger base may not necessarily be the same shape as a finger tip, but, in addition to the last assumption, let us assume that the tip extends as far ahead of a corresponding stable displacement as the base lags behind. Equation (16) then suggests that the positions of the tip and base of a finger could be given by

$$x_t = v[t + k' \ln (1 + k'' e^{t/k'})], \quad x_b = v[t - k' \ln (1 + k'' e^{t/k'})]. \tag{17}$$

Here the premise that $\lim_{t\to\infty} dx_b/dt = 0$ is included, which becomes true as $M_1/M_2 \to \infty$, i.e. under such conditions the base of the finger eventually becomes stationary. Inspection of figure 3 indicates the extent to which this occurs. In the radial situation with constant injection rate, the average radius grows as the square root of time; hence the equations for the tip of a finger $r_t$ and the base of a finger $r_b$ become of the form

$$r_t = (Q/\pi)^{\frac{1}{2}}[t + k' \ln(1 + k'' e^{t/k'})]^{\frac{1}{2}}, \tag{18a}$$

$$r_b = (Q/\pi)^{\frac{1}{2}}[t - k' \ln(1 + k'' e^{t/k'})]^{\frac{1}{2}}. \tag{18b}$$

3.2.2. *Comparison with experiment.* Using $Q = 9{\cdot}3\,\mathrm{cm}^2/\mathrm{s}$, (18*b*) was fitted to three of the finger bases from the pattern in figure 3. Least-squares fits for $k'$ and $k''$ gave $k' = 4{\cdot}0 \pm 1{\cdot}0\,\mathrm{s}$. This suggested that $k'$ was essentially a constant in this experiment and, as a consequence, was assigned the value $4{\cdot}0\,\mathrm{s}$. $k''$ was then determined by letting the limit of (18*b*), namely $(-Qk' \ln k''/\pi)^{\frac{1}{2}}$, become equal to the experimentally determined position of the finger bases at large $t$. The values of $k''$ were thus determined as 0·12, 0·038 and 0·0040. The solid lines in figure 4 were obtained when these values were inserted in (18*b*), showing a reasonable fit to the data points. Persisting with $k' = 4{\cdot}0\,\mathrm{s}$, it remained to find a system that would generate a range of $k''$ that would fit all the finger bases. Bearing in mind the result of (13), a given number of fingers can only occur after a certain radius has been exceeded. Furthermore, it appeared in figure 3 that the fingers had wavelength $\lambda_m$ around the time of their inception and, as they developed, their wavelength became longer than $\lambda_m$. This led to the surmise that fingers occur at the integer steps of $\epsilon n_m$ where $\epsilon$ is to be determined and $n_m$ is given by (14). Moreover, as each finger occurred, let it have had fixed amplitude $\xi = R - r_b$ to start with. Figure 5 is a plot of the number of finger bases encountered within radius $r$. A visual fit between the experiment of figure 3 (broken line) and the above theory (solid line) was obtained with $\epsilon = 0{\cdot}7$ and $\xi = 0{\cdot}6\,\mathrm{cm}$. $\epsilon$ determines the slope of the theoretical curve and $\xi$ determines the horizontal displacement. A phenomenon to note is that bubble growth is comparatively close to circular until the circumference divides up into about 8 fingers.

Figure 6 was compiled with $\epsilon = 0{\cdot}7$, $\xi = 0{\cdot}6\,\mathrm{cm}$, $Q = 9{\cdot}3\,\mathrm{cm}^2/\mathrm{s}$ and $k' = 4{\cdot}0\,\mathrm{s}$. The solid line corresponds to the radius of a stable displacement and the dashed lines are the positions of the finger bases. The diamonds indicate the radii at which each additional finger occurs.

Some remarks can be made here on the finite-sized perturbation required for the instability to show a significant effect in finite time. A first reaction might be to postulate that perturbations are probably the size of a pore in a porous medium and, by analogy, would be roughly the magnitude of the plate spacing in a Hele Shaw cell. Perturbations are caused by inhomogeneities and the significant inhomogeneities on the surface of the glass of the Hele Shaw cell are probably variations in wettability. If there is a very small region of surface wet with fluid 1 and an adjoining very small region wet with fluid 2, then the interface will flex or jump a distance of the order of the plate spacing even though these 'very small' regions may be far less than the plate spacing. To compile figure 5, a perturbation of 4·0 times the plate spacing was used, and the author believes this is large. The author also believes that $\epsilon = 0{\cdot}7$ is small. These values compensate each other and it is concluded that (18) may not work well when amplitudes are small. Deeper investigation may resolve these difficulties.

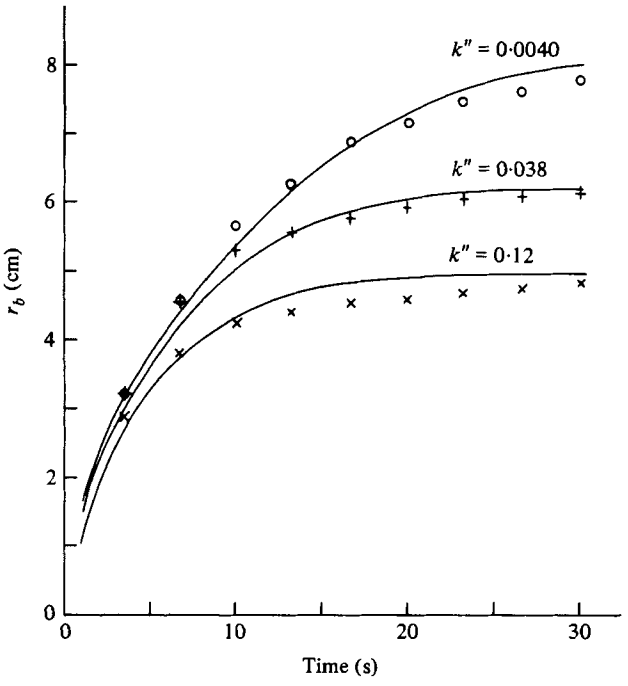


FIGURE 4. The positions of the finger bases with time. The solid lines are given by

$$r_b = 1{\cdot}7\{t - 4{\cdot}0 \ln [1{\cdot}0 + k'' \exp (t/4{\cdot}0)]\}^{\frac{1}{2}},$$

where $k'$ has been given the value 4·0 and $k''$ = 0·12, 0·038 and 0·0040. The data points are the positions of three of the finger bases from figure 3.

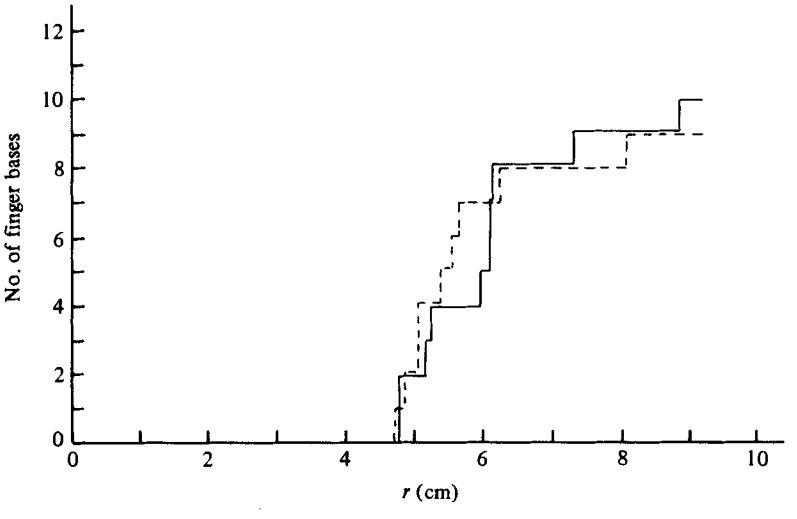


FIGURE 5. The number of finger bases encountered within radius $r$ at large $t$. The broken line is from the experiment shown in figure 3. The solid line is derived with the theory in the text.

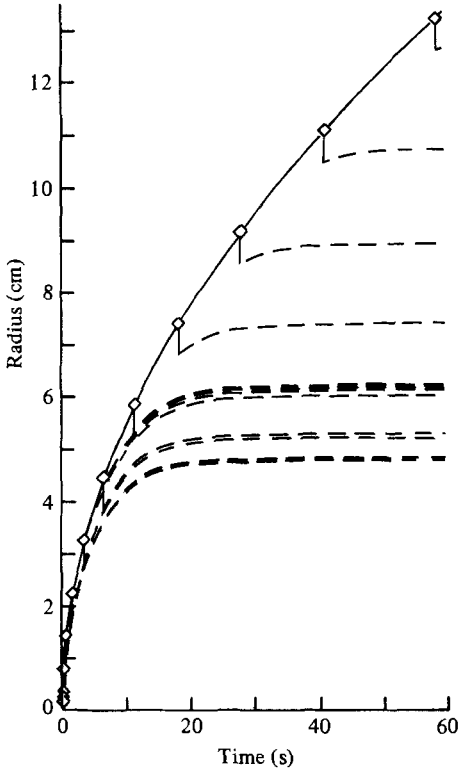


FIGURE 6. An example which gives the positions of the finger bases based on the theory in the text. The solid line corresponds to a stable displacement with $R = 1{\cdot}7\sqrt{t}$. The diamonds indicate points at which a given number of fingers $n$ can occur, where $n$ is equal to the integral part of $0{\cdot}7[\frac{1}{3}(65R+1)]^{\frac{1}{2}}$. The dashed lines correspond to the positions of the finger bases given by

$$r_b = 1{\cdot}7\{t - 4{\cdot}0 \ln [1{\cdot}0 + k'' \exp (t/4{\cdot}0)]\}^{\frac{1}{2}},$$

where $k''$ is generated by $R - r_b = 0{\cdot}6$ at the corresponding diamond.

### 3.3. *Quasi-infinite fingers*

In order to derive an equation for the bubble surface of an infinitely long finger in a linear displacement, Saffman & Taylor (1958) consider a uniform flow where the potential function $\phi$ and the stream function $\psi$ are given by

$$\phi = Vx \quad \text{and} \quad \psi = Vy. \tag{19}$$

They then transform from the $x$, $y$ plane into the $\phi$, $\psi$ plane and superimpose perturbations so that

$$y = \frac{\psi}{v} + \sum_{m=1}^{\infty} A \sin \frac{m\pi\psi}{v} \exp\left(\frac{-m\pi\phi}{v}\right). \tag{20}$$

The coefficients $A_m$ are calculated to satisfy the boundary conditions,

$$A_m = 2(-1)^m (1-\Gamma)/m\pi, \tag{21}$$

after which the equation for the bubble surface is determined. If the origin of coordinates is taken to be the tip of the finger then this equation is (Taylor & Saffman 1959)

$$x = \frac{2}{\pi}(1-\Gamma) \ln (\cos \pi y/2\Gamma). \tag{22}$$

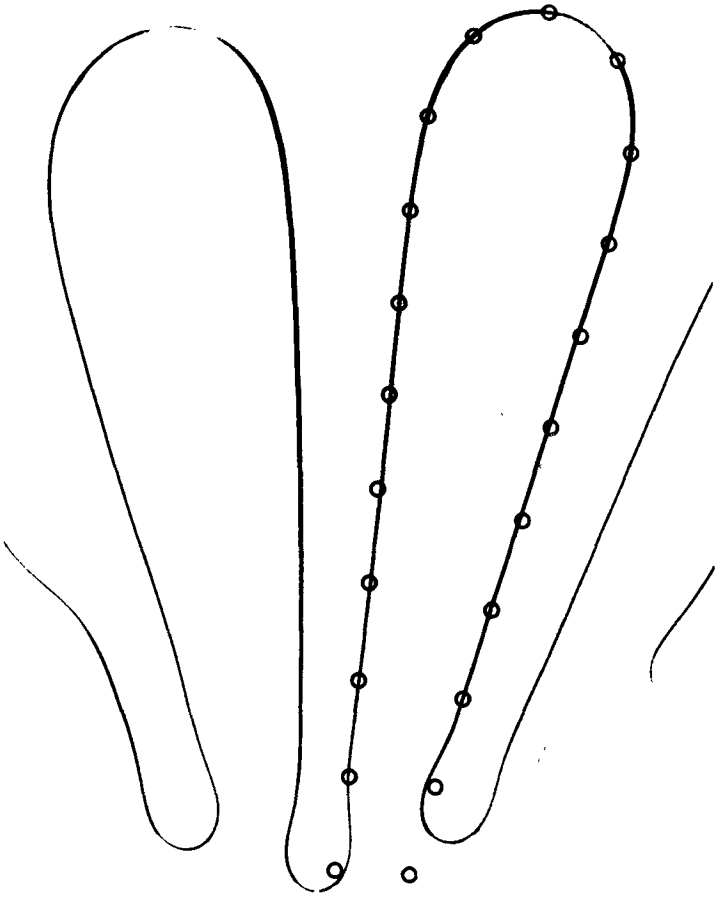

FIGURE 7. The curve $(r/r_t)^{18} = \cos 15\theta$ (small circles) compared with a finger resulting from the injection of air into a Hele Shaw cell filled with glycerine.

If, instead of considering a uniform flow, one considers a point source, then

$$\phi = \frac{-Q}{2\pi} \ln r \quad \text{and} \quad \psi = \frac{-Q}{2\pi} \theta. \tag{23}$$

By transforming from the $r$, $\theta$ plane into the $\phi, \psi$ plane, perturbations can be superimposed to give (20). The boundary conditions are the same as for Saffman & Taylor's analysis except that there is an additional condition that there be an integral number of fingers in a circumference. Thus the equation

$$\ln r = \frac{1-\Gamma}{\pi} \ln \frac{1}{2}\left(1 + \cos \frac{n\theta}{2}\right) \tag{24}$$

can be derived, although $\Gamma$ loses some meaning owing to $\lambda$ being a function of $r$ and the ability of the fingers to split. By setting $\frac{1}{2}\pi/(1-\Gamma)$ equal to $\alpha$, (24) can be rearranged to give

$$(r/r_t)^{\alpha} = \cos n\theta, \tag{25}$$

with $\alpha$ and $n$ to be determined, as the equation for the finger. This equation has been empirically fitted to a finger giving $\alpha = 18$ and $n = 15$ and this is shown in figure 7. Fingers can also be asymmetric (Taylor & Saffman 1959). Figure 8 illustrates such a finger.

FIGURE 8. An asymmetric finger.

### 3.4. *Extended growth: splitting of fingers*

As the radius of the bubble increases, the fingers become wider until they exceed two critical wavelengths. At this stage they become unstable and bifurcate (figure 9). This process repeats itself indefinitely as the radius grows larger and larger and a 'tree-like' structure is created as the fingers 'branch off'.

## 4. Inward fingering

Attention is now focused on the complementary case, corresponding to withdrawal of oil from a well. This situation begins with the more viscous fluid closer to the well. For simplicity, only the case of an initially circular interface is considered. Two sets of fluids were examined: experiments with glycerine and air gave the most photographic contrast; experiments with glycerine and oil gave continued recovery after the less viscous fluid had reached the well. In both cases the glycerine corresponded to oil in the practical situation and the air or oil corresponded to ground water. This simulation can be made so long as there is a large viscosity difference between the fluids so that the viscosity of the less viscous fluid can be ignored. A pattern which resulted from the withdrawal of glycerine from a Hele Shaw cell otherwise filled with air is shown in figure 10. The initially circular interface was achieved through the stable displacement of air by glycerine.

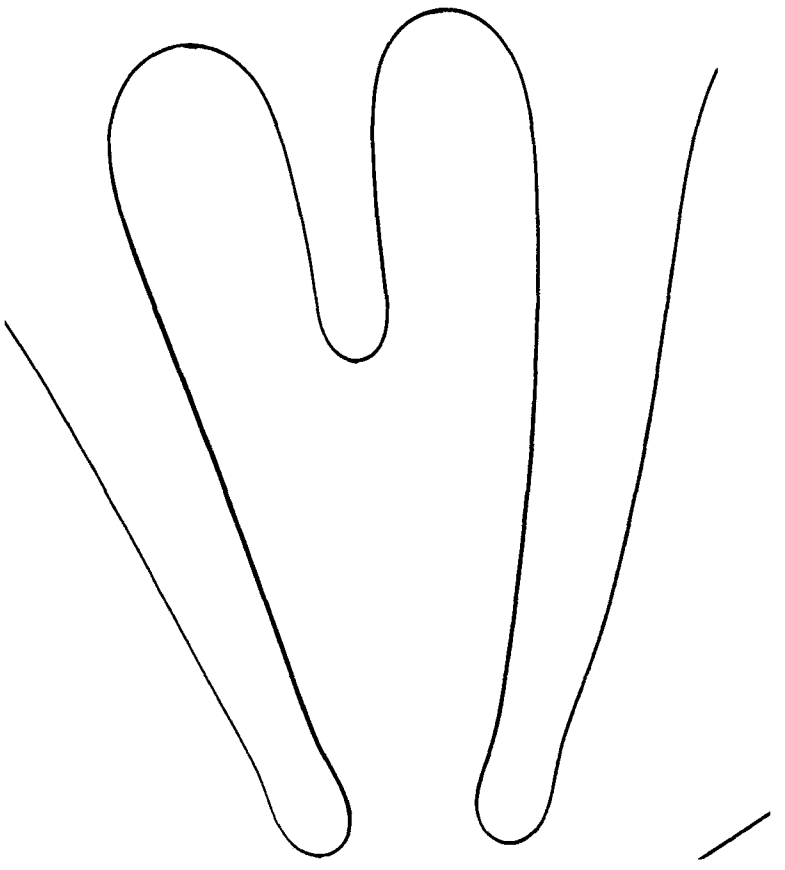

FIGURE 9. A finger bifurcating.

### 4.1. *Initial growth*

The Hele Shaw cell experiments began with an initially circular interface contracting inwards and experiencing perturbations due to inhomogeneities, such as variations in wettability, on the surface of the glass plates. Analysis of the initial perturbation is essentially the same for withdrawal as for injection, except that, when the approximation $M_1 \ll M_2$ is made in (10),

$$n_c = \left(\frac{|Q|R}{2\pi\sigma M_1} + \tfrac{1}{4}\right)^{\frac{1}{2}} + \tfrac{1}{2} \tag{26}$$

is obtained instead of (11).

$$n_m = \left[\frac{1}{3}\left(\frac{|Q|R}{2\pi\sigma M_1} + 1\right)\right]^{\frac{1}{2}} \tag{27}$$

remains essentially unchanged.

As for injection, the initially circular interface begins to finger with the number of fingers governed by the number of times $\lambda$ divides the circumference. It appears in figure (10) that this value of $\lambda$ is slightly less than $\lambda_m$. This could correspond to the same mechanism which causes the finger wavelength to become larger than $\lambda_m$ for outward fingering as the fingers become significant.

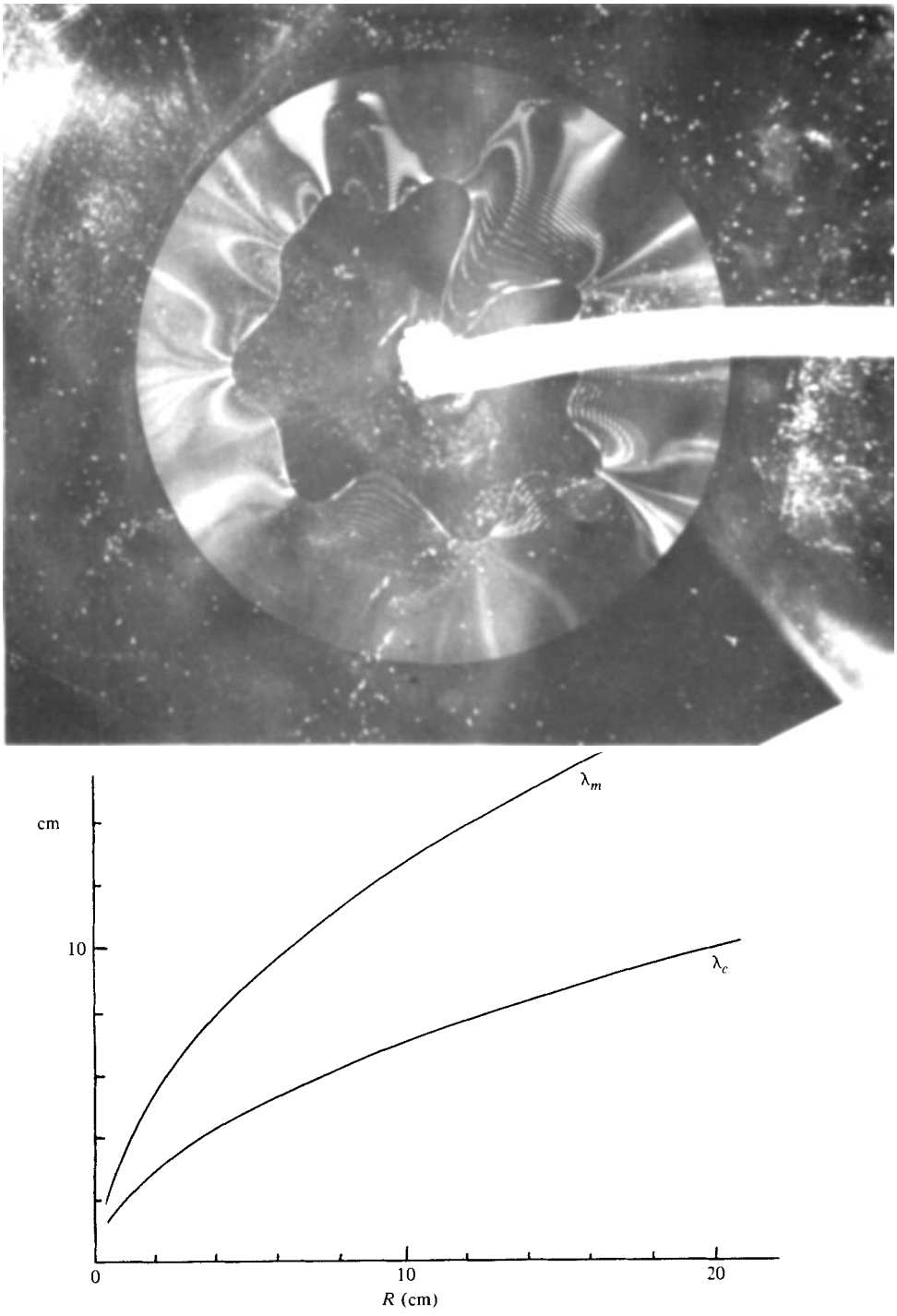


FIGURE 10. A multiple exposure photograph of the pattern which occurs during the withdrawal of glycerine from a Hele Shaw cell otherwise filled with air.

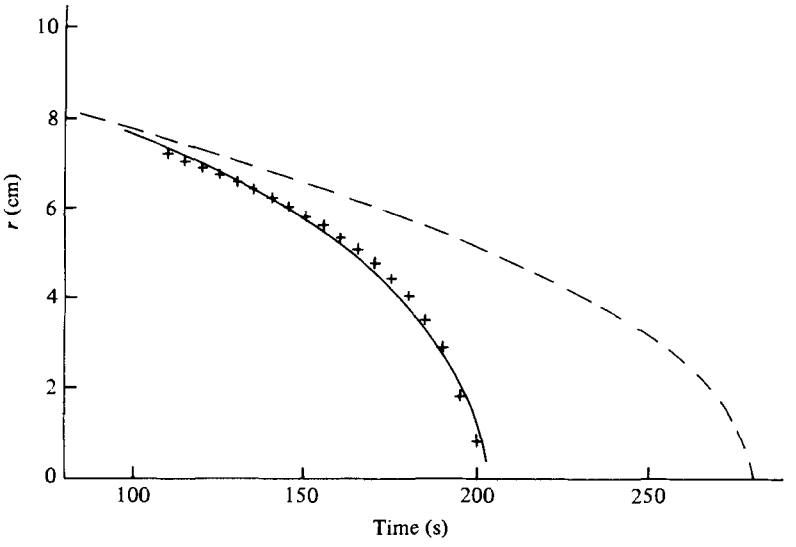


FIGURE 11. The position of a finger tip against time. The broken line is the average position of the interface given by $R = 0{\cdot}58(280-t)^{\frac{1}{2}}$. The solid line is the position of the finger tip given by: $r_t = 0{\cdot}58\{280-t-20\ln[1{\cdot}0+0{\cdot}0020\exp(t/20)]\}^{\frac{1}{2}}$. The data points + indicate the position of the dominant finger in figure 10.

### 4.2. *Intermediate growth*

As the interface contracts, (26) indicates that the number of allowable fingers decreases. The smaller fingers have their growth impeded while the more established fingers continue to grow. Eventually one finger dominates and accelerates into the well (refer to figure 10). If the average radius of the interface is given by (4), the growth equation can be reversed to give

$$r_t = (|Q|/\pi)^{\frac{1}{2}}[t_0-t-k'\ln(1+k''e^{t/k'})]^{\frac{1}{2}}. \tag{28}$$

With $Q = 1{\cdot}04\,\mathrm{cm}^2/\mathrm{s}$ and $t_0 = 280\,\mathrm{s}$, this is shown graphically in figure 11 where the broken line represents the average position of the interface and the solid line represents the position of the tip of an unimpeded finger given by (28) with $k' = 20$ and $k'' = 0{\cdot}0020$. The plus signs indicate the position of the dominant finger in figure (10).

If siphoning is used to withdraw the fluids and one of the fluids is gas, then the siphon ceases to function soon after the gas reaches the well. However, if two liquids are used, then withdrawal continues after a finger has reached the well so that more fingers will converge into the well. The finger bases begin to assume the shape of the quasi-infinite fingertips associated with injection.

During the phase beginning with the penetration of a finger to the well, i.e. where two liquids are being withdrawn simultaneously, the volume flow rates depend on the viscosities and the ratios of the segments subscribed by each liquid. An example of the ratio of individual fluids recovered to the total volume of glycerine recovered is given in figure 12. Extending the analogy to flow in porous media and oil recovery, this would mean that ground water would appear in the recovered oil in increasing amounts. Nevertheless, considering only fingering, all the oil would still be recovered if one were prepared to pump for long enough. (However, in practice, a large fraction of the oil is unrecoverable owing to other mechanisms such as residual saturation.)

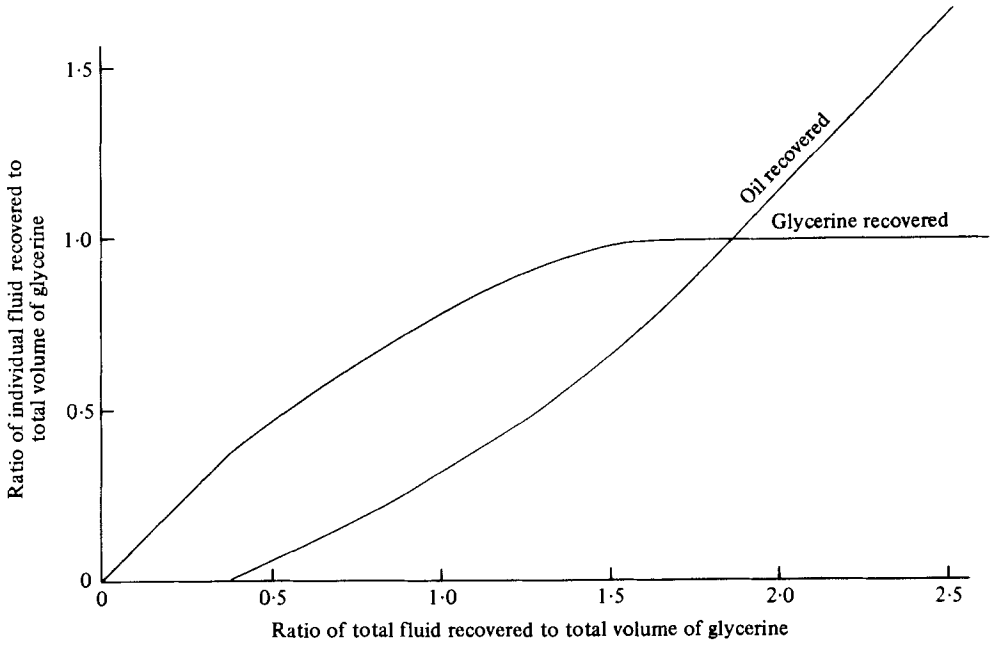


FIGURE 12. Individual fluids recovered plotted against total fluid recovered during withdrawal when glycerine is enclosed by oil.

### 4.3. *Quasi-infinite fingers*

A finger resulting from the withdrawal of glycerine from a Hele Shaw cell otherwise filled with oil is shown in figure 13. The withdrawal has been continued after the oil has reached the well, so at this stage both fluids are being withdrawn simultaneously. The equation

$$(r/r_b)^\alpha = \cos n\theta, \tag{29}$$

derived in § 3.3, has been empirically fitted to the finger in figure 13 giving $\alpha = 6$ and $n = 6$, and is shown by the small circles.

## 5. Conclusion

Radial fingering in a circular Hele Shaw cell has been observed and described for both the injection and withdrawal of fluids. The significant points are the verification of a preferred wavelength of finger, the derivation of the form of the growth of fingers and the derivation of an equation to fit long fingers. Within the analysis there are certainly sections which would benefit from mathematical analysis at a deeper level. Nevertheless, it is to be hoped that these experiments will aid predictions on such things as how a gas bubble injected into a confined aquifer will behave, although it still remains to establish fingering as a real phenomenon in reservoir conditions.

The author wishes to thank R. A. Wooding for his elucidation of the linear stability analysis upon which § 3.1 is based. The author also wishes to express his appreciation of O. M. Williams's comments during the preparation of this paper.

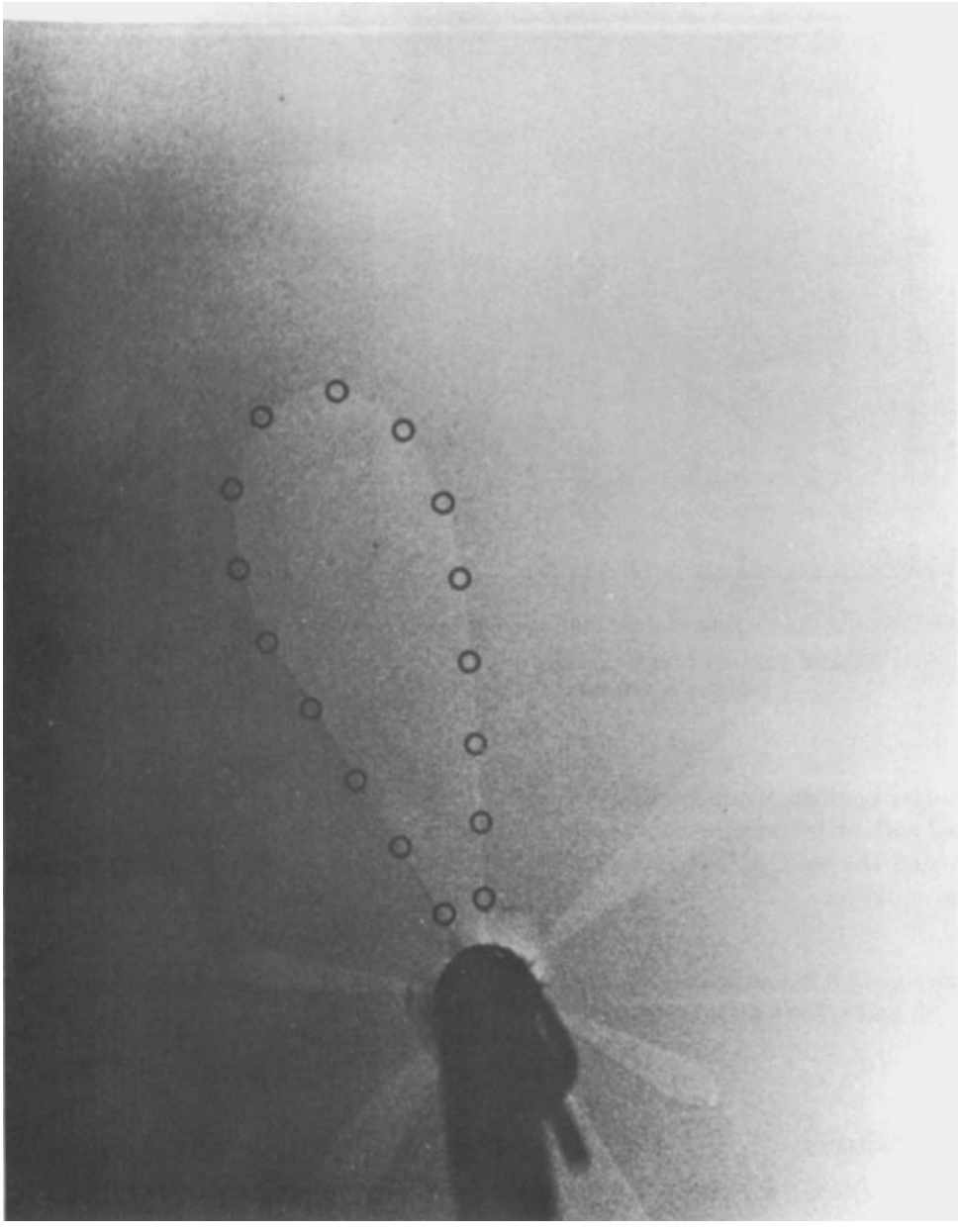

FIGURE 13. The curve $(r/r_b)^6 = \cos 6\theta$ (small circles) compared with a finger resulting from the withdrawal of glycerine from a Hele Shaw cell otherwise filled with oil.

## REFERENCES


BATAILLE, J. 1968 *Revue Inst. Pétrole*, **23**, 1349–1364.

BEAR, J. 1972 *Dynamics of Fluids in Porous Media*. Elsevier.

CARDEN, P. O. & PATERSON, L. 1979 *Int. J. Hydrogen Energy*, **4**, 559–569.

CHUOKE, R. L., VAN MEURS, P. & VAN DER POEL, C. 1959 *Trans. A.I.M.E.* **216**, 188–194.

GUPTA, S. P., VARNON, J. E. & GREENKORN, R. A. 1973 *Water Resour. Res.* **9**, 1039–1046.

HABERMANN, B. 1960 *Trans. A.I.M.E.* **219**, 264–272.

PATERSON, L. 1980 The implications of fingering in underground hydrogen storage. In *Proc. 3rd World Hydrogen Energy Conference, Tokyo, June* 23–26. Pergamon Press.

PITTS, E. 1980 *J. Fluid Mech.* **97**, 53–64.

POLLARD, D. D., MULLER, O. H. & DOCKSTAD, D. R. 1975 *Geol. Soc. Am. Bull.* **86**, 351–363.

RICHARDSON, J. G. 1961 In *Handbook of Fluid Dynamics* (ed. V. L. Streeter). McGraw-Hill.

ROARK, R. J. 1965 *Formulas for Stress and Strain*, 4th edn. McGraw Hill.

SAFFMAN, P. G. & TAYLOR, G. I. 1958 *Proc. Roy. Soc.* A **245**, 312–329.

SAFFMAN, P. G. 1959 *Quart. J. Mech. Appl. Math.* **12**, 146–150.

SCHEIDEGGAR, A. E. 1960*a* *Phys. Fluids*, **3**, 94–104.

SCHEIDEGGAR, A. E. 1960*b* *Can. J. Phys.* **38**, 153–162.

SETTARI, A., PRICE, H. S. & DUPONT, T. 1977 *Soc. Pet. Eng. J.* June, 228–246.

TAYLOR, G. I. & SAFFMAN, P. G. 1959 *Quart. J. Mech. Appl. Math.* **12**, 265–279.

VAN MEURS, P. 1957 *Trans. A.I.M.E.* **210**, 295–301.

WHITE, I., COLOMBERA, P. M. & PHILIP, J. R. 1976 *Soil Sci. Soc. Am. J.* **40**, 824–829.

WILSON, S. D. R. 1975 *J. Colloid Interface Sci.* **51**, 532–534.

WOODING, R. A. 1969 *J. Fluid Mech.* **39**. 477–495.

WOODING, R. A. & MOREL-SEYTOUX, H. 1976 *Ann. Rev. Fluid Mech.* **8**, 233–274.